Nuclear Engineering and Technology 52 (2020) 889–896

Contents lists available at ScienceDirect

Nuclear Engineering and Technology

journal homepage: www.elsevier.com/locate/net

Original Article

Investigation on reverse flow characteristics in U-tubes under two-phase natural circulation

Xi Chu, Mingrui Li, Wenzhen Chen[*,1], Jianli Hao

College of Nuclear Science and Technology, Naval University of Engineering, Wuhan, 430033, PR China

ARTICLE INFO

Article history:
Received 15 May 2019
Received in revised form
3 September 2019
Accepted 14 October 2019
Available online 17 October 2019

Keywords:
Two-phase natural circulation
Reverse flow
UTSG
U-tubes

ABSTRACT

The vertically inverted U-tube steam generator (UTSG) is widely used in the pressurized water reactor (PWR). The reverse flow behavior generally exists in some U-tubes of a steam generator (SG) under both single- and two-phase natural circulations (NCs). The behavior increases the flow resistance in the primary loop and reduces the heat transfer in the SG. As a consequence, the NC ability as well as the inherent safety of nuclear reactors is faced with severe challenges. The theoretical models for calculating single- and two-phase flow pressure drops in U-tubes are developed and validated in this paper. The two-phase reverse flow characteristics in two types of SGs are investigated base on the theoretical models, and the effects of the U-tube height, bending radius, inlet steam quality and primary side pressure on the behavior are analyzed. The conclusions may provide some promising references for SG optimization to reduce the disadvantageous behavior. It is also of significance to improve the NC ability and ensure the PWR safety during some accidents.

1. Introduction

The passive safety technology is widely considered in the third generation of nuclear power plant (NPP). Using the technology, the reactor can carry out the corresponding safety functions without the human intervention and external power supply during an accident [1].

After the Three Mile Island accident in 1979, the physical phenomena and thermal hydraulic behaviors in the reactor coolant system during the small break loss of coolant accident (SBLOCA) have gradually become the focus of reactor safety research in various countries [2]. During the SBLOCA in a pressurized water reactor (PWR), the reactor will shut down and the main pumps may stop running. Due to the decreases of pressure and coolant inventory in the primary loop, the steam may generate in the reactor hot leg or core, and the single- and two-phase natural circulations (NCs) as well as the reflux condensation flow modes successively become the effective ways to transport the decay heat from the core to the secondary side of steam generator (SG) [3]. The changes of these flow modes and the related system parameters were experimentally investigated in many thermal hydraulic test facilities, such as the SEMISCALE Mod-2A [4], LOBI [5,6], LSTF [7], PKL [8], BETHSY [9], PACTEL [3] and IIST [10]. The studies showed that the reverse flow behavior generally existed in some U-tubes of SG under both single-phase and two-phase NCs. The reverse flow will increase the flow resistance in the primary loop and reduce the heat transfer in the SG. As a consequence, the NC ability as well as the inherent safety of nuclear reactor is faced with severe challenges.

Sanders [11] developed a theoretical analysis model for single-phase NC flow in the U-tube, and the unstable solutions of all parallel U-tubes were obtained. The mechanism of single-phase reverse flow was interpreted by the small perturbation theory. Hao et al. [12,13] studied the influence of U-tube length on the single-phase reverse flow. And the critical points of this behavior in the SG were measured by the experiment. Based on the homogeneous flow model, Jeong et al. [14] formulated a mathematical model to study the two-phase flow and heat transfer characteristics in parallel U-tubes. A judgment criterion of reverse flow in U-tubes under the two-phase NC was obtained, and its physical explanation was also given. Chu et al. [15] used RELAP5/MOD 3.3 program to study the influence factors of the two-phase reverse flow in U-tubes under the low steam quality condition.

The characteristics and influence factors of single-phase reverse flow in SGs have been well studied. However, the special and in-

* Corresponding author.
E-mail address: Cwz2@21cn.com (W. Chen).
[1] Present address: Faculty 304, College of Nuclear Science and Technology, Naval University of Engineering, Wuhan, 430033, PR China.

https://doi.org/10.1016/j.net.2019.10.012

depth studies on the two-phase reverse flow are still insufficient. The existing researches mainly use simple homogeneous flow model, and its conclusions can only be applied to the bubble flow with a low steam quality in U-tubes. To this end, this paper develops the theoretical models to calculate the single- and two-phase flow pressure drops in U-tubes. Base on the models, the two-phase reverse flow characteristics are investigated. Besides, the effects of the U-tube height, bending radius, inlet steam quality and primary side pressure on the behavior are analyzed.

2. Theoretical models

The single- or two-phase reverse flow in U-tubes, also known as the flow excursion, belongs to the category of static flow instability. The primary work to study this behavior is to accurately calculate the pressure drop between the U-tube inlet and outlet [14]. When the steam-water two-phase fluid enters the U-tubes, the steam phase may be totally condensed as liquid water. Alternatively, the U-tubes outlet may still be the two-phase flow with a certain steam quality due to the insufficient condensation. As shown in Fig. 1, it is assumed that the lengths of single- and two-phase segments are L_{sp} and L_{tp}, respectively, the U-tube height is H, the one-dimensional coordinate position in the flow direction is s, and the bending radius of the U-tube is R_u. The U-tube length L can be written as follows:

$$L = L_{tp} + L_{sp} = 2H + \pi R_u \tag{1}$$

The total pressure drop can be expressed as follows [16]:

$$\Delta p = \Delta p_f + \Delta p_g + \Delta p_r + \Delta p_a \tag{2}$$

where Δp_f, Δp_g, Δp_r, and Δp_a denote the pressure drops due to friction, gravitation, local resistance and acceleration, respectively. The calculating methods of them are described below.

2.1. Friction pressure drop

The friction pressure gradient of single-phase flow can be expressed as follows [16]:

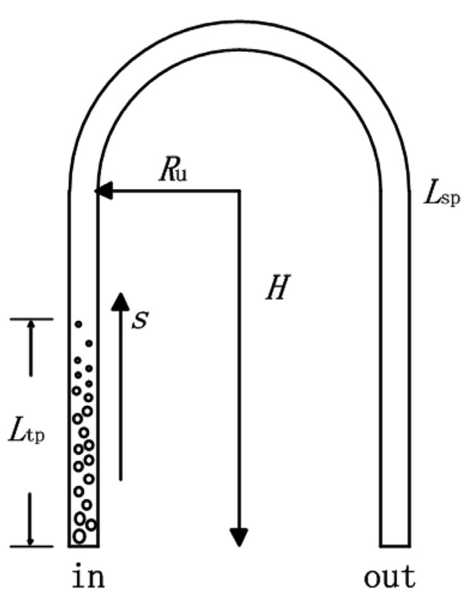

Fig. 1. Schematic of U-tube.

$$-\left(\frac{dp_f}{ds}\right)_{sp} = \frac{f_{sp} G^2}{2\rho_{sp} d_i} \tag{3}$$

where f_{sp} is the friction coefficient of single-phase flow; G is the mass velocity, kg/(m^2·s); ρ_{sp} is the single-phase flow density, kg/m^3; d_i is the U-tube inner diameter, m.

The friction pressure gradient of two-phase flow can be expressed as that of single-phase flow multiplying a two-phase friction multiplier [17]:

$$-\left(\frac{dp_f}{ds}\right)_{tp} = -\left(\frac{dp_f}{ds}\right)_{lo} \varphi_{lo}^2 = -\left(\frac{dp_f}{ds}\right)_{go} \varphi_{go}^2 \tag{4}$$

$$-\left(\frac{dp_f}{ds}\right)_{tp} = -\left(\frac{dp_f}{ds}\right)_{l} \varphi_{l}^2 = -\left(\frac{dp_f}{ds}\right)_{g} \varphi_{g}^2 \tag{5}$$

where $-(dp_f/ds)_{lo}$ and φ_{lo}^2 are the friction pressure gradient and the multiplier if the liquid water flows in the same U-tube with the mass flux equal to that of the total steam-water mixture, respectively. Similarly, $-(dp_f/ds)_{go}$ and φ_{go}^2 are those if the steam flows in the same U-tube with the mass flux equal to that of the total steam-water mixture, respectively. $-(dp_f/ds)_l$ and φ_l^2 denote the friction pressure gradient and the multiplier if the liquid water of the mixture flows alone in the same U-tube. Similarly, $-(dp_f/ds)_g$ and φ_g^2 denote those if the steam of the mixture flows alone in the same U-tube.

Friedel [18] proposed an experimental correlation to calculate φ_{lo}^2 for the bubble or slug flow, which can be expressed as follows:

$$\varphi_{lo}^2 = (1-x)^2 + \frac{x^2 \rho_l f_{go}}{\rho_g f_{lo}} + \frac{3.24 x^{0.78} (1-x)^{0.24}}{\mathrm{Fr}^{0.045} \mathrm{We}^{0.035}} \left(\frac{\rho_l}{\rho_g}\right)^{0.91} \left(\frac{\mu_g}{\mu_l}\right)^{0.19} \left(1 - \frac{\mu_g}{\mu_l}\right)^{0.7} \tag{6}$$

where ρ_l and ρ_g are the water and steam densities, respectively, kg/m^3; μ_l and μ_g are the dynamic viscosities of the water and steam, respectively, kg/(m·s); f_{go} and f_{lo} are the friction coefficients if the steam and the liquid water flow in the same U-tube with the mass flux equal to that of the total mixture, respectively; Fr and We are the Froude number and Weber number of the two-phase flow, respectively, which can be written as follows:

$$\mathrm{Fr} = \frac{G^2}{g d_i \rho_{tp}^2} \tag{7}$$

$$\mathrm{We} = \frac{G^2 d_i}{\sigma \rho_{tp}^2} \tag{8}$$

where σ is the surface tension coefficient, N/m^2.

For the annular flow, φ_g^2 can be expressed as follows [17]:

$$\varphi_g^2 = \left[\frac{1 + 75(1-\alpha)}{\alpha^{2.5}}\right] \times \left(1 + E\frac{(1-x)}{x}\right) \left\{1 - \left[\frac{2\alpha\rho_g (1-x)(1-E)}{\rho_l x (1-\alpha)}\right]\right\}^2 \tag{9}$$

where α is the void fraction; E is the entrainment rate, it represents how much liquid water is carried in the steam core.

The transition boundary between bubble/slug flow and annular flow was given by Ref. [19] as:

$$\frac{j_g \rho_g^{0.5}}{[g(\rho_l - \rho_g)\sigma]^{0.25}} = 3.09 \tag{10}$$

where j_g is the steam superficial velocity, m/s; g is the gravitational acceleration, m/s^2.

The void fraction in the U-tube can be calculated by the following correlations proposed by Ref. [20]:

$$\alpha = \frac{x\varepsilon_\alpha}{1 + (\varepsilon_\alpha - 1)x} \tag{11}$$

$$\varepsilon_\alpha = 1.5\left(\frac{\rho_l}{\rho_g}\right)^{0.692} - 0.5 \tag{12}$$

where ε_α is the slip factor.

2.2. Gravitation pressure drop

The gravitation pressure gradient of single- or two-phase flow in the U-tube can be expressed as follows [16]:

$$-\frac{dp_g}{ds} = \rho g \sin\theta \tag{13}$$

where ρ is the fluid density, kg/m^3; θ is the horizontal angle, rad. From Eq. (13) it can be found that the crucial work of calculating Δp_g is to obtain the fluid density.

The two-phase density in the U-tube can be written as follows:

$$\rho_{tp} = \alpha\rho_g + (1-\alpha)\rho_l \tag{14}$$

Based on the thermal equilibrium assumption, the steam quality along the U-tube can be written as follows [15]:

$$x(s) = \frac{h(s) - h_l}{h_{lg}} \tag{15}$$

where h is the two-phase specific enthalpy, J/kg; subscripts l and g denote the saturated water and saturated steam, respectively; h_{lg} is the latent heat of vaporization, $h_{lg} = h_g - h_l$.

The two-phase energy conservation equation in the U-tube is:

$$-GA\frac{dh}{ds} = P\alpha_{tp}\Delta T \tag{16}$$

where A is the flow area, m^2; P is the wetted perimeter, m; ΔT is the fluid temperature difference between the U-tube primary side and secondary side, K; $\Delta T = T_{s1} - T_{s2}$, T_{s1} is the saturated temperature of the primary side, T_{s2} is the secondary side temperature; α_{tp} is the total heat transfer coefficient between the primary side and secondary side when the fluid in the U-tube is two-phase, W/(m^2·K).

Integrating Eq. (16) from the U-tube inlet ($s = 0$, $h = h_{in}$) to s ($s < L_{tp}$), the two-phase specific enthalpy can be obtained as follows:

$$h(s) = h_{in} - \frac{P\alpha_{tp}\Delta T}{AG}s \tag{17}$$

where h_{in} is the inlet specific enthalpy, J/kg. Substituting Eq. (17) into Eq. (15) results in:

$$x(s) = x_{in} - \frac{\xi_2\Delta T}{G}s \tag{18}$$

where $\xi_2 = \frac{P\alpha_{tp}}{Ah_{lg}}$; x_{in} is the inlet steam quality. Substituting Eq. (18) into Eq. (11), the void fraction along the U-tube can be obtained, then the two-phase density ρ_{tp} can be given according to Eq. (14). Substituting $x(s) = 0$ into Eq. (18), the two-phase segment length L_{tp} also can be obtained as follows:

$$L_{tp} = \frac{x_{in}G}{\xi_2\Delta T} \tag{19}$$

The single-phase density can be expressed as a function of temperature based on the Boussinesq assumption [12]:

$$\rho_{sp} = \rho_0[1 - \beta(T - T_{s2})] \tag{20}$$

where ρ_0 is the reference density, which can be assigned as the density corresponding to the SG secondary side temperature; β is the thermal expansion coefficient, K^{-1}; T is the single-phase temperature, K.

The single-phase energy conservation equation in the U-tube is:

$$\frac{\partial T}{\partial s} = -\frac{P\alpha_{sp}(T - T_{s2})}{AGc_p} \tag{21}$$

where c_p is the specific heat, J/(kg·K); α_{sp} is the total heat transfer coefficient between the primary side and secondary side when the fluid in the U-tube is single-phase, W/(m^2·K).

Integrating Eq. (21) from the initial point of single-phase segment ($s = L_{tp}$, $T = T_{s1}$) to s ($s \geq L_{tp}$) results in:

$$T(s) = T_{s2} + (T_{s1} - T_{s2})e^{-\frac{\xi_1}{G}(s - L_{tp})} \tag{22}$$

where $\xi_1 = \frac{P\alpha_{sp}}{Ac_p}$.

Substituting Eq. (22) into Eq. (20), the single-phase density ρ_{sp} can be obtained.

2.3. Local resistance and acceleration pressure drops

The local resistance pressure drop of single-phase flow in the U-tube bending part can be calculated by the following correlation [16]:

$$\Delta p_{r,sp} = K\frac{G^2}{2\rho_{sp}} \tag{23}$$

where K is the local resistance coefficient, which can be expressed as follow:

$$K = \left[0.262 + 0.326\left(\frac{d_i}{R_u}\right)^{3.5}\right]\frac{\phi}{\pi} \tag{24}$$

where ϕ is the bending angle, rad.

The local resistance pressure drop of two-phase flow in the U-tube bending part can be written as follows:

$$\Delta p_{r,tp} = \Delta p_{r,lo}\left\{1 + \left(\frac{\rho_l}{\rho_g} - 1\right)\left[\frac{2}{K}x(1-x)\Delta\left(\frac{1}{S}\right) + x\right]\right\} \tag{25}$$

where $\Delta p_{r,lo}$ is the local resistance pressure drop if the total mixture flows as liquid water in the same U-tube, Pa; $\Delta\left(\frac{1}{S}\right)$ is known as the velocity ratio increment of steam to water, which can be expressed as follows [21]:

$$\Delta\left(\frac{1}{S}\right) = \frac{1.1}{2 + R_u/d_i} \tag{26}$$

If the U-tube outlet steam quality is greater than 0 (x_{out}>0), the acceleration pressure drop can be expressed as:

$$\Delta p_a = G^2\left\{\left[\frac{(1-x_{out})^2}{\rho_l(1-\alpha_{out})}+\frac{x_{out}^2}{\rho_g\alpha_{out}}\right]-\left[\frac{(1-x_{in})^2}{\rho_l(1-\alpha_{in})}+\frac{x_{in}^2}{\rho_g\alpha_{in}}\right]\right\} \quad (27)$$

If $x_{out} = 0$, the acceleration pressure drop can be expressed as:

$$\Delta p_a = G^2\left\{\frac{1}{2\rho_{out}}+\frac{1}{2\rho_l}-\left[\frac{(1-x_{in})^2}{\rho_l(1-\alpha_{in})}+\frac{x_{in}^2}{\rho_g\alpha_{in}}\right]\right\} \quad (28)$$

3. Model validation

In section 2, the theoretical models for calculating single- and two-phase flow pressure drops in U-tubes are developed. They will be validated in this section using two groups of experiments. One is the SG single-phase flow instability experiment performed by us [13], and the other is the two-phase boiling experiment in a NC loop conducted by Ref. [22].

As shown in Fig. 2, the SG single-phase flow instability test facility consists of coolant pump, electrical heater, SG simulator, pressurizer, several valves, pipes, and measuring devices such as flow meter, thermocouple and pressure difference transmitter. The working fluid is the deionized water. There are 18 U-tubes with different lengths in the SG simulator. A target flow meter is installed in the entrance of SG simulator. Some K-type thermocouples are fixed at the inlet and outlet of the U-tubes and SG simulator to measure the fluid temperatures. A pressure difference transmitter is fixed around one U-tube to measure the pressure difference between its entrance and exit.

The pressure and mass flow rate in the primary loop were maintained at 3Mpa and 0.9 t/h, respectively. The primary fluid was gradually heated by increasing the heating rate. The heating process was terminated when the reverse flow behavior in the SG simulator was judged by the temperature signals.

A medium length U-tube is taken as the research object, its outlet temperature and pressure drop are calculated by the theoretical models developed in this paper, and the comparisons of the calculating values with the experiment data are shown in Figs. 3 and 4. From Figs. 3 and 4, it can be seen that the models can precisely calculate the U-tube outlet temperatures and pressure drops with a reasonable error range.

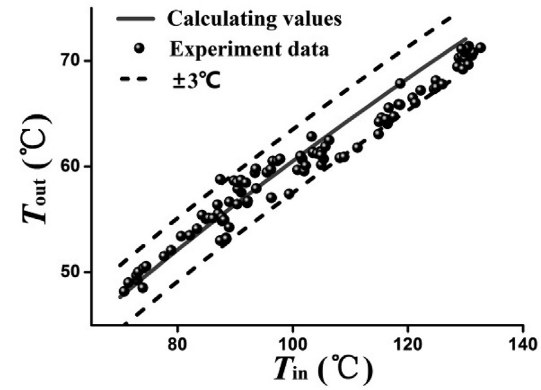

Fig. 3. Comparison of outlet temperature between calculation and experiment.

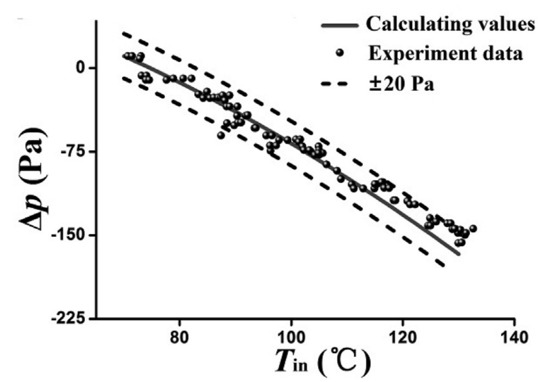

Fig. 4. Comparison of single-phase flow pressure drop between calculation and experiment.

In different experiments, the single-phase reverse flow critical points were measured, which were critical inlet temperature $\Delta T_{in,\,c}$ and mass flow rate M_c. Using the theoretical models, they are also calculated. The calculating values and experiment data are compared in Fig. 5. It can be found that the models can well predict the single-phase reverse flow critical points of the SG simulator.

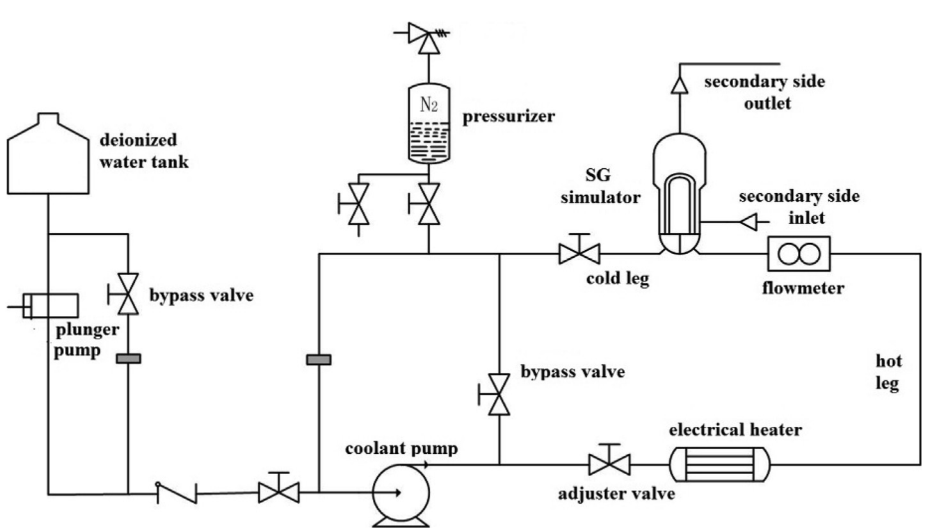

Fig. 2. SG single-phase flow instability test facility.

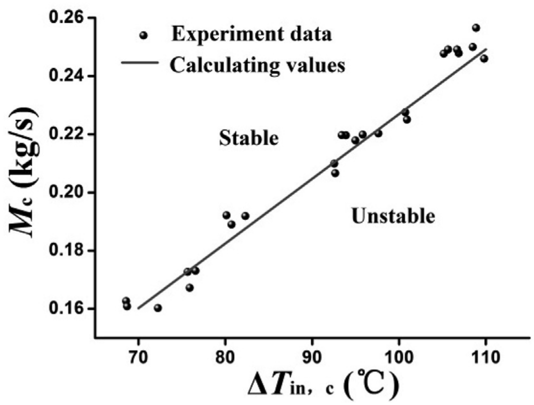

Fig. 5. Comparison of reverse flow critical point of SG between calculation and experiment.

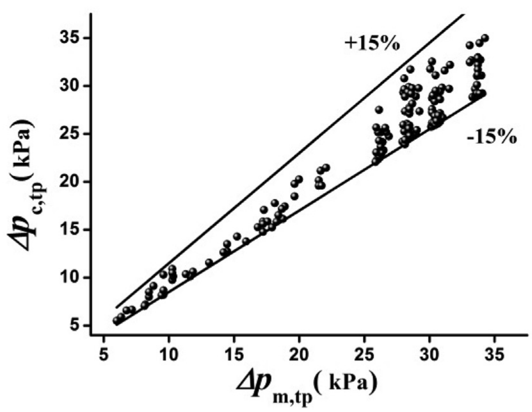

Fig. 6. Comparison of two-phase flow pressure drop between calculation and experiment.

Jain [22] designed a two-phase NC test loop to study the effects of the inner diameter, inlet subcooling degree and pressure on the two-phase flow instability in a vertical boiling tube. The pressure drops between the tube inlet and outlet were measured in the experiments. Based on the experimental conditions, the pressure drops are also calculated using the theoretical models developed in this paper. The comparison of the calculating results $\Delta p_{c,\,tp}$ with the measuring data $\Delta p_{m,\,tp}$ is shown in Fig. 6. It can be found that the models also can be used to calculate the two-phase flow pressure drop in a tube.

4. Two-phase reverse flow analyses

Two types of SGs are chosen as the research object. The parameters of the U-tubes are shown in Table 1. Type A is a typical small marine SG used in ship NPP, and type B is a big commercial SG used in LSTF test facility [7].

The equations introduced in Section 2 are numerically calculated using MATLAB software. The U-tube is divided into a number of segments. In a fluid differential unit Δs, all of the pressure drops are calculated. After the sensitivity analysis, the most appropriate segment quantity is confirmed on the premise of acceptable computation speed and enough accuracy ($\Delta p \leq 0.001$ Pa). Fig. 7 shows the variations of Δp, Δp_f, Δp_g, Δp_r and Δp_a with mass velocity in U-tubes under a general two-phase NC. It can be seen that the local resistance pressure drop Δp_r and the acceleration pressure drop Δp_a are respectively positive and negative, both of them have almost no effect on the total pressure drop Δp. Δp is mainly determined by Δp_f and Δp_g. Due to a non-monotonic change of the gravitation pressure drop with the mass velocity, Δp curve has a remarkable negative slope region (AO segment in Fig. 7). Once the mass velocity decreases from point B to point O (the inflection point), reverse flow may occur in the U-tube. The AO segment is the flow instability region and it usually does not exist in the stable flow state. The mass velocity and pressure drop corresponding to the point O were called as the critical mass velocity G_c and the critical pressure drop Δp_c [14]. If the practical G and Δp are lower than their critical values, normal flow will be difficult to continue.

Considering that the parallel U-tubes in a SG work in the same practical pressure drop before the reverse flow occurrence, from Fig. 7 it can be seen that flow in the U-tube with greater Δp_c will be reversed firstly when the mass velocity drops from point B to point O. Thus Δp_c determines the reverse flow distribution in the SG. Due to the different practical mass velocities in different U-tubes, G_c cannot be used to judge the reverse flow distribution, but it is the crucial parameter of the flow instability boundary of the SG. If G_c is too great, the reverse flow will be most likely to occur in the SG even if the total inlet mass velocity is relatively great.

The effects of the U-tube height, bending radius, inlet steam quality and primary side pressure on Δp_c and G_c are discussed as follows.

4.1. Effects of U-tube height and bending radius

The effect of U-tube length on the reverse flow under single-phase NC was studied by Refs. [12]. [14,15] investigated its effects under two-phase NC with low steam quality (x_{in}<0.1). As a further study, the theoretical model developed in this paper extends the inlet mass quality to a greater range ($x_{in} = 0\text{–}1$) to respectively study the effects of the U-tube height and bending radius.

For the different inlet mass qualities, Figs. 8 and 9 show the variations of critical pressure drop and mass velocity with the U-

Table 1
Parameters of SG U-tubes.

Parameter	Value	
	Type A	Type B
U-tube height, m	H_0	9.44–10.644
Bending radius, mm	R_{u0}~12.6 R_{u0}	51–311
Inner diameter, mm	d_{i0}	19.6
Outer diameter, mm	d_{o0}	25.4
Normal operation pressure in primary side, MPa	14	15.6
Normal operation pressure in secondary side, MPa	p_{s0}	6.5

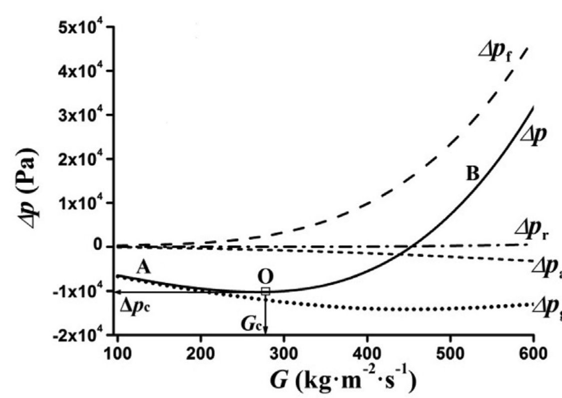

Fig. 7. Variation of pressure drop with mass velocity.

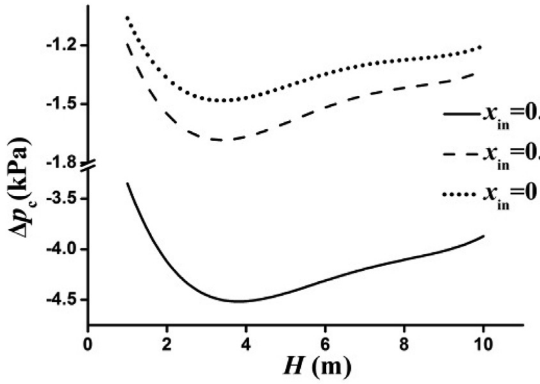

Fig. 8. Variation of critical pressure drop with U-tube height.

tube height, respectively. It can be found that the minimum Δp_c and maximum G_c will appear when H is about 3–4 m. Since the U-tube heights of SG A are usually lower than 3 m, and the U-tube heights of SG B are higher than 9 m, with the increase of H, Δp_c of SG A will decrease and G_c of SG A will increase no matter what the inlet mass quality is. However, the variations of Δp_c and G_c with H for the SG B are totally contrary compared with the SG A.

Figs. 10 and 11 show the variations of Δp_c with the bending radius under single- and two-phase NCs, respectively. It can be seen that the change rules of Δp_c with R_u are different for various U-tube heights. For the SG A, the U-tube with smaller R_u has a greater Δp_c because of the low U-tube height. On the contrary, for the SG B, the U-tube with greater R_u has a greater Δp_c because of the high U-tube height. The variations of Δp_c with R_u in the U-tube are the same for both single- and two-phase NCs. Because G_c is the crucial parameter of the flow instability boundary for different SGs, and R_u is not the main distinction among them, the variation of G_c with R_u is not discussed here.

4.2. Effect of inlet steam quality

Figs. 12–15 give the variations of critical pressure drop and mass velocity with the inlet steam quality for the U-tubes in SGs A and B, respectively. Figs. 12 and 13 show that Δp_c approximately linearly decreases with the increase of x_{in} no matter what the SG is. From Figs. 14 and 15, it can be seen that G_c linearly increases firstly and then exponentially decreases with the increase of x_{in}. The change rule of G_c with x_{in} under the low steam quality is totally different with that under the high steam quality.

It can be concluded that because of the higher Δp_c, the reverse

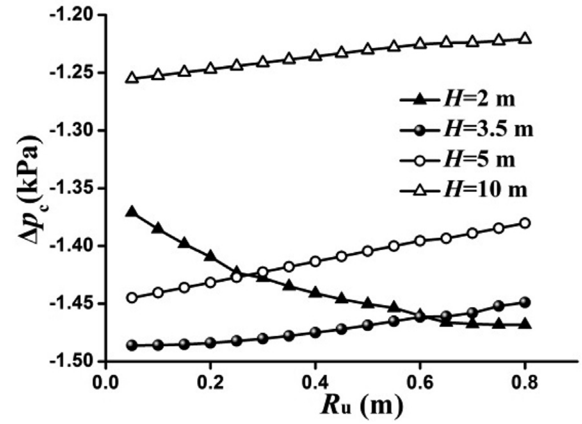

Fig. 10. Variation of critical pressure drop with bending radius under single-phase NC.

flow is more likely to occur in the U-tube with smaller inlet steam quality for the parallel U-tubes in the same SG. But for different SGs, the risk of reverse flow occurrence will increase firstly and then decrease with the increase of x_{in}, which is similar to the change of G_c.

4.3. Effect of primary side pressure

During the SBLOCA, the primary side pressure p will dramatically decrease with the development of the accident. Thus it is significant to analyze its effects on the reverse flow in the SG. Figs. 16–19 give the variations of critical pressure drop and mass velocity with p for the U-tubes in SGs A and B, respectively. p_0 is the normal operation pressure in the primary side (see Table 1).

Figs. 16–19 show that under the low inlet steam quality condition ($x_{in} = 0.05$), Δp_c increases firstly and then decreases with p and G_c decreases firstly and then increases. However, under the high inlet steam quality condition ($x_{in} = 0.5$), the change rules of Δp_c and G_c with p are completely opposite to that under the low inlet steam quality condition.

5. Conclusions

The theoretical models for calculating single- and two-phase flow pressure drops in U-tubes are developed. Using SG single-phase flow and two-phase NC experiment data, the models are validated. The two-phase reverse flow characteristics in two types of SGs are investigated by the theoretical models, and the effects of

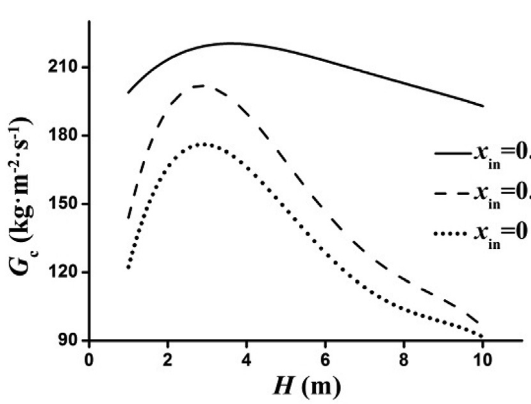

Fig. 9. Variation of critical mass velocity with U-tube height.

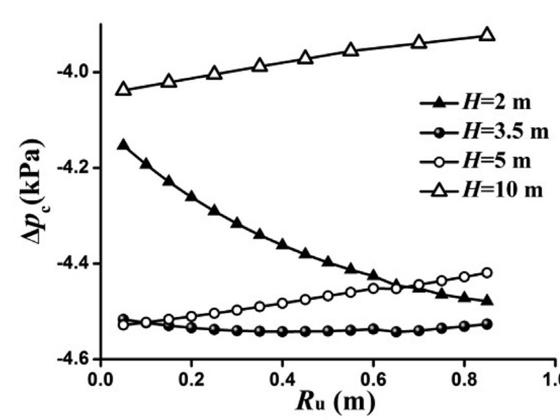

Fig. 11. Variation of critical pressure drop with bending radius under two-phase NC.

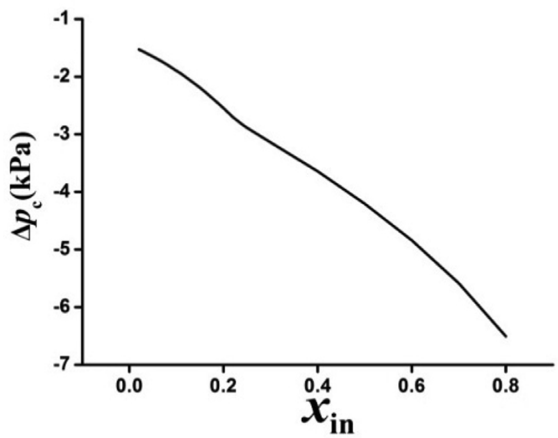

Fig. 12. Variation of critical pressure drop with inlet steam quality for U-tubes in SG A.

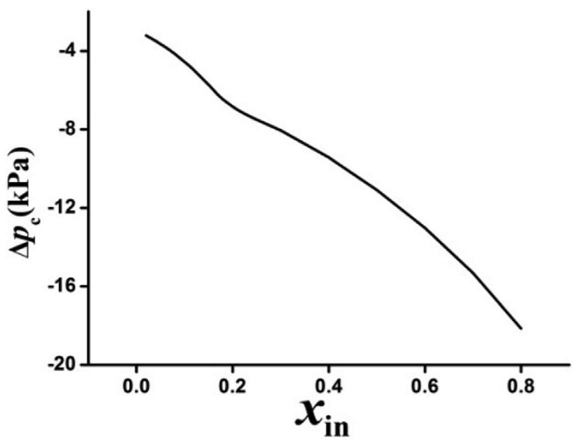

Fig. 13. Variation of critical pressure drop with inlet steam quality for U-tubes in SG B.

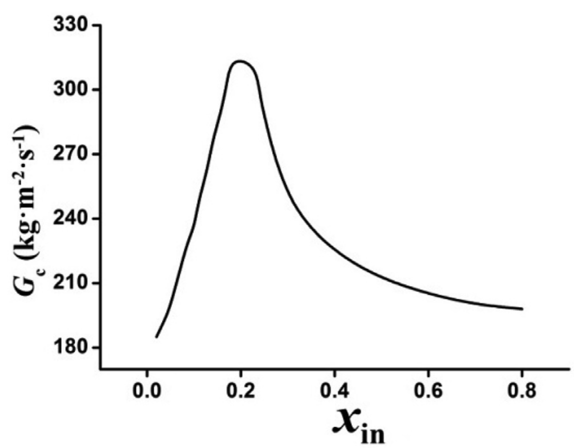

Fig. 14. Variation of critical mass velocity with inlet steam quality for U-tubes in SG A.

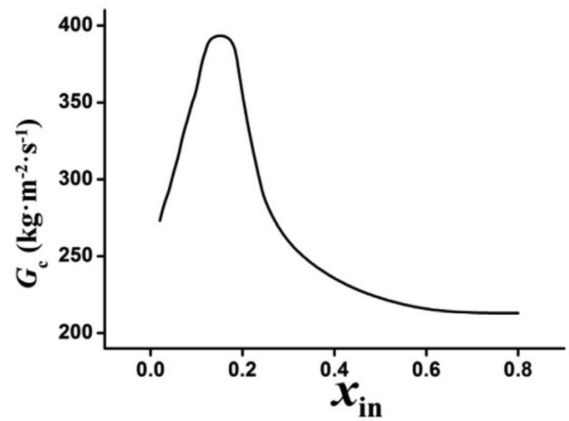

Fig. 15. Variation of critical mass velocity with inlet steam quality for U-tubes in SG B.

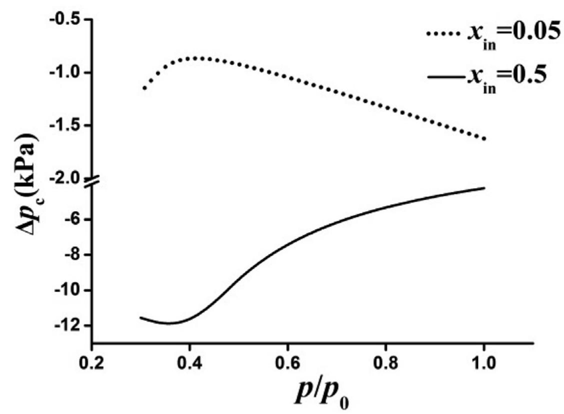

Fig. 16. Variation of critical pressure drop with primary side pressure for U-tubes in SG A.

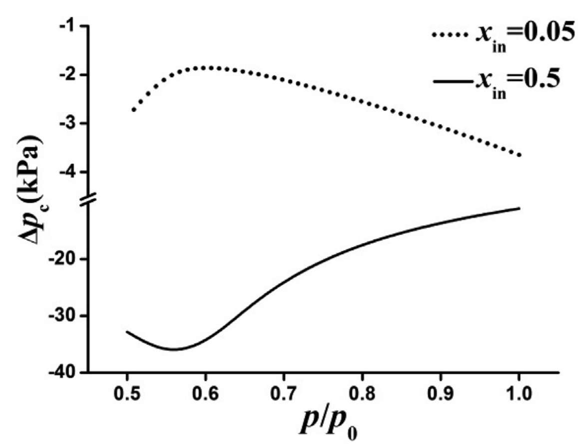

Fig. 17. Variation of critical pressure drop with primary side pressure for U-tubes in SG B.

U-tube height, bending radius, inlet steam quality and primary side pressure on the critical pressure drop Δp_c and critical mass velocity G_c are analyzed. The main conclusions can be summarized as follows:

(1) Due to a non-monotonic change of the gravitation pressure drop with the mass velocity in the U-tube, Δp curve has a remarkable negative slope region and the reverse flow may occur. The flow in the U-tube with greater Δp_c will be reversed firstly when the mass velocity drops. Thus Δp_c determines the reverse flow distribution in the SG. And G_c is the crucial parameter of the SG flow instability boundary. The

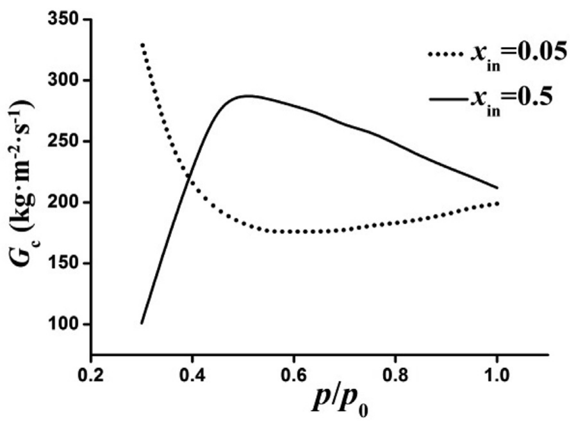

Fig. 18. Variation of critical mass velocity with primary side pressure for U-tubes in SG A.

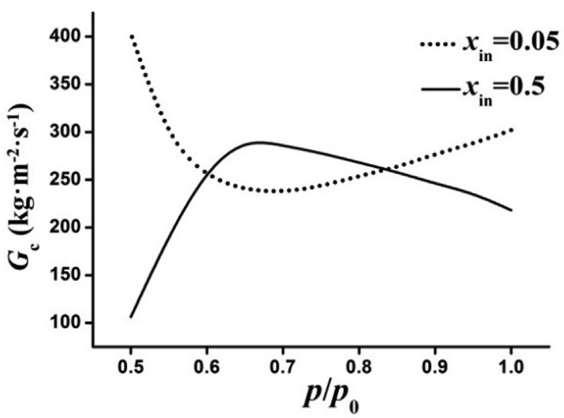

Fig. 19. Variation of critical mass velocity with primary side pressure for U-tubes in SG B.

reverse flow will be most likely to occur in the SG with the great G_c.

(2) The minimum Δp_c and maximum G_c will appear when the U-tube height H is about 3–4 m. With the increase of H, Δp_c of the small marine SG (SG A) decreases and its G_c increases no matter what the inlet mass quality is. However, the variations of Δp_c and G_c with H for the big commercial SG (SG B) are totally contrary.

(3) For the small marine SG, the U-tube with smaller R_u has a greater Δp_c because of the low U-tube height. On the contrary, for the big commercial SG, the U-tube with greater R_u has a greater Δp_c because of the high U-tube height. The change rules of Δp_c with R_u in the U-tube are the same for both single- and two-phase NCs.

(4) The two-phase reverse flow is more likely to occur in the U-tube with smaller inlet steam quality for parallel U-tubes in the same SG. But for different SGs, with the increase of x_{in}, the risk of reverse flow occurrence will increase firstly and then decrease.

(5) Under the low inlet steam quality condition, with the decrease of the primary side pressure, Δp_c increases firstly and then decreases, and G_c decreases firstly and then increases. However, the change rules of Δp_c and G_c with the primary side pressure under the high inlet steam quality condition are completely opposite.

Acknowledgements

This research was financially supported by the National Natural Science Foundation of China (project number 11402300 and 11502298).

Appendix A. Supplementary data

Supplementary data to this article can be found online at https://doi.org/10.1016/j.net.2019.10.012.

References

[1] Z.J. Yang, J.Q. Shan, J.L. Gou, Preliminary assessment of a combined passive system for typical 3-loop PWR CPR1000, Nucl. Eng. Des. 313 (2017) 141–161.
[2] K. Kawanishi, A. Tsuge, M. Fujiwara, Experimental study on heat removal during cold leg small break LOCAs in PWRs, J. Nucl. Sci. Technol. 28 (6) (1991) 555–569.
[3] V. Kouhia, V. Riikonen, O.P. Kauppinen, Benchmark exercise on SBLOCA experiment of PWR PACTEL facility, Ann. Nucl. Energy 59 (2013) 149–156.
[4] S.N. Kim, W.H. Jang, The simulation of Semiscale natural circulation test S-NC-3, S-NC-4 using RELAP 5/Mod 3.1, J. Korean Nucl. Soc. 30 (5) (1998) 424–434.
[5] F. D'Auria, G.M. Galassi, Flowrate and density oscillations during two-phase natural circulation in PWR typical conditions, Nucl. Eng. Des. 122 (1990) 209–218.
[6] G.F. De Santi, F. Mayinger, Steam condensation and liquid holdup in steam generator U-tubes during oscillatory natural circulation, Exp. Heat Transf. 6 (1993) 367–387.
[7] Y. Kukita, H. Nakamura, K. Tasaka, Nonuniform steam generator U-tube flow distribution during natural circulation tests in ROSA-IV large scale test facility, Nucl. Sci. Eng. 99 (1988) 289–298.
[8] B. Schoen, P. Weber, Nitrogen in a steam generator of a PWR under SBLOCA conditions: experimental investigations in the PKL test facility and comparison with analytical studies, Exp. Therm. Fluid Sci. 15 (1997) 238–252.
[9] Y.J. Chung, H.C. Kim, M.H. Chang, Post test analysis to natural circulation experiment on the BETHSY facility using the MARS 1.4 code, J. Korean Nucl. Soc. 33 (6) (2001) 638–651.
[10] Y.M. Ferng, C.H. Lee, Numerical simulation of natural circulation experiments conducted at the IIST facility, Nucl. Eng. Des. 148 (1994) 119–128.
[11] J. Sanders, Stability of single-phase natural circulation with inverted U-tube steam generators, J. Heat Transf. 110 (1988) 735–742.
[12] J.L. Hao, W.Z. Chen, D. Zhang, Effect of U-tube length on reverse flow in UTSG primary side under natural circulation, Ann. Nucl. Energy 56 (2013) 66–70.
[13] J.L. Hao, W.Z. Chen, G.J. Hu, X. Chu, D. Zhang, L. Yu, Experimental research on reverse flow critical point among parallel U-tubes in SG, Prog. Nucl. Energy 98 (2017) 59–70.
[14] J.J. Jeong, M. Hwang, Y.J. Lee, B.D. Chung, Non uniform flow distribution in the steam generator U-tubes of a pressurized water reactor plant during single and two-phase natural circulations, Nucl. Eng. Des. 231 (2004) 303–314.
[15] X. Chu, W.Z. Chen, J.L. Hao, D. Zhang, Investigation on reverse flow phenomenon in UTSGs under two-phase natural circulation with low steam quality, Ann. Nucl. Energy 119 (2018) 1–6.
[16] W.Z. Chen, L. Yu, J.L. Hao, Thermal Hydraulics of Nuclear Power Plants, Chinese Atomic Energy Press, Beijing, 2013 (in Chinese).
[17] G.B. Wallis, One-dimensional Two-phase Flow, McGraw Hill Book Co., New York City, 1969.
[18] L. Friedel, Improved Friction Pressure Drop Correlations for Horizontal and Vertical Two-phase Pipe Flow, European Two-Phase Flow Group Meet, Ispra, Italy, 1979.
[19] Y. Taitel, A.E. Dukler, Flow Regime Transition for Vertical Upward Gas-Liquid Flow, in: AICHE 70th Annual Meeting, 1979. New York).
[20] J.R.S. Thom, Prediction of pressure drop during forced circulation boiling of water, Int. J. Heat Mass Transf. 7 (1964) 709–724.
[21] D. Chisholm, Two-phase flow in bends, Int. J. Multiph. Flow 6 (4) (1980) 363–367.
[22] K.C. Jain, Self-sustained Hydrodynamic Oscillations in a Natural-Circulation Two-Phase-Flow Boiling Loop, Argonne National Laboratory Report, 1965. ANL-7073.